PERIÓDICO TCHÊ QUÍMICA
ARTIGO ORIGINAL

MÉTODO NUMÉRICO PARA DETERMINAR A DEPENDÊNCIA DO ESTADO DE TENSÃO TÉRMICA DA HASTE DA TEMPERATURA DO MEIO AMBIENTE NA PRESENÇA SIMULTÂNEA DE PROCESSOS TÉRMICOS

A NUMERICAL METHOD FOR DETERMINING THE DEPENDENCE OF THE THERMALLY STRESSED STATE OF A ROD ON AMBIENT TEMPERATURE WITH THE SIMULTANEOUS PRESENCE OF THERMAL PROCESSES

ЧИСЛЕННЫЙ МЕТОД ОПРЕДЕЛЕНИЯ ЗАВИСИМОСТИ ТЕРМОНАПРЯЖЕННОГО СОСТОЯНИЯ СТЕРЖНЯ ОТ ТЕМПЕРАТУРЫ ОКРУЖАЮЩЕЙ СРЕДЫ ПРИ ОДНОВРЕМЕННОМ НАЛИЧИИ ТЕПЛОВЫХ ПРОЦЕССОВ

MYRZASHEVA, Aigul N.[1]; KENZHEGULOV, Beket[2*]; SHAZHEDEKEEVA, Nurgul K.[3]; TULEUOVA, Raigul U.[4];

[1,2,3,4]Atyrau State University named after Kh. Dosmukhamedov, Department of Mathematics and Methods of Teaching Mathematics, 1 Studenchesky Ave., zip code 060011, Atyrau – Republic of Kazakhstan

** Correspondence author*
e-mail: b.kenzhegulov@asu.edu.kz

Received 12 May 2020; received in revised form 06 June 2020; accepted 19 June 2020

RESUMO

Os métodos existentes para estudar o estado termicamente deformado e tenso de uma haste de comprimento limitado feita de liga especial resistente ao calor não levam em conta a presença simultânea de processos térmicos, como transferência de calor, força axial, isolamento térmico, temperatura local, condições operacionais da haste e o fato, que em larga escala o coeficiente de expansão térmica do material da haste depende de temperatura. Para resolver esses problemas, os autores propõem um novo método numérico para estudar o estado termomecânico de uma haste de comprimento limitado feita da liga resistente ao calor ANV-300. Esta haste é de comprimento limitado e rigidamente comprimida com duas extremidades. A superfície lateral das seções $(0 \le x \le L/3)$ e $(2L/3 \le x \le L)$ o núcleo são isolados termicamente. No local $(L/3 \le x \le 2L/3)$ da haste, é fornecida a temperatura local, que varia em coordenada por uma lei linear. Os estudos foram realizados em diferentes temperaturas ambientes. Os padrões da distribuição do campo de deslocamentos elásticos do componente elástico da deformação são construídos de acordo com a lei de Hooke, com os valores do componente elástico da tensão e levando em consideração a dependência do campo entre o coeficiente de expansão térmica e temperatura. Como resultado do estudo, verificou-se que uma mudança na temperatura da área transversal da extremidade esquerda do ambiente tem um efeito menor no estado de tensão térmica da haste considerada do que o efeito da mudança.

Palavras-chave: *minimização da energia potencial, método dos elementos finitos, isolamento térmico, temperatura, coeficiente de transferência de calor.*

ABSTRACT

Existing methods for studying the thermally stressed and deformed state of a rod of the limited length from a special heat-resistant alloy do not take into account the simultaneous presence of thermal processes, such as heat exchange, axial force, thermal insulation, local temperature, operating conditions of the rod and the full-scale dependence of the coefficient of thermal expansion of the material of the rod on temperature. To solve such problems, the authors propose a new numerical method for studying the thermomechanical state of a rod of the limited length from the heat-resistant alloy ANV-300. This rod is of a limited length and rigidly clamped at both ends. The lateral surface of sections $(0 \le x \le L/3)$ and $(2L/3 \le x \le L)$ of the rod is thermally insulated. At the site $(L/3 \le x \le 2L/3)$ of the rod, the local temperature is given, which varies in coordinate by a linear law. The studies were carried out at different ambient temperatures. The laws of the distribution field of elastic displacements of the elastic component of deformation are constructed, respectively, according to Hooke's law, the values of the elastic component of stress, taking into account the field dependence between the coefficient of thermal expansion and temperature. As a result of studies, it was found that a change in the temperature of the

DOI: 10.52571/PTQ.v17.n35.2020.65_MYRZASHEVA_pgs_765_780.pdf

surrounding cross-sectional area of the left end of the medium has little effect on the thermally stressed state of the considered rod than the effect of the change.

Keywords: *minimization of potential energy, finite element method, thermal insulation, temperature, heat transfer coefficient.*

АННОТАЦИЯ

Существующие методы исследования термически напряженного и деформированного состояния стержня ограниченной длины из специального жаропрочного сплава не учитывают одновременное наличие тепловых процессов, таких как теплообмен, осевая сила, теплоизоляция, локальная температура, условия эксплуатации стержня и натурная зависимость коэффициента теплового расширения материала стержня от температуры. В статье на основе минимизаций потенциальной энергии упругих деформаций с применением метода квадратичного конечного элемента с тремя узлами разработана математическая модель термонапряженно-деформированного состояния горизонтального стержня из жаропрочного сплава АНВ-300. Данный стержень ограниченной длины и жестко защемлен с двумя концами. Боковая поверхность участков $(0 \le x \le L/3)$ и $(2L/3 \le x \le L)$ стержня теплоизолированная. На участке $(L/3 \le x \le 2L/3)$ стержня дана локальная температура, меняющаяся по координате линейным законом. Через площадь поперечных сечений обоих концов данного стержня происходит тепловой обмен с окружающими их средами. Закономерности распределения поля упругих смещений упругой составляющей деформации строятся в соответствии с законом Гука, значениями упругой составляющей напряжений с учетом полевой зависимости между коэффициентом теплового расширения и температурой. В результате исследования было установлено, что изменение температуры окружающей площади поперечного сечения левого конца среды оказывает меньшее влияние на термически напряженное состояние рассматриваемого стержня, чем влияние изменения.

Ключевые слова: *минимизация потенциальной энергии, метод конечных элементов, теплоизоляция, температура, коэффициент теплообмена.*

1. INTRODUCTION

The influence of ambient temperature on the thermally stressed state of a rod of this alloy in the presence of local temperature is carried out, and numerical results of the study are presented. Ambient temperature affects the rod through the cross-section of the left end. The studies were carried out at different ambient temperatures. The laws of the distribution field of elastic displacements of the elastic component of deformation are constructed, respectively, according to Hooke's law, the values of the elastic component of stress, taking into account the field dependence between the coefficient of thermal expansion and temperature. As a result of studies, it was found that a change in the temperature of the surrounding cross-sectional area of the left end of the medium has little effect on the thermally stressed state of the considered rod than the effect of the change. Thus, only by changing the value (and not), i.e., by changing the environmental properties of the surrounding cross-sectional area where heat transfer occurs, the thermally stressed state of the rod under investigation can be changed.

Existing methods for studying the thermally stressed and deformed state of a rod of the limited length from a special heat-resistant alloy do not take into account the simultaneous presence of thermal processes, such as heat exchange, axial force, thermal insulation, local temperature, operating conditions of the rod and the full-scale dependence of the coefficient of thermal expansion of the material of the rod on temperature (Geng *et al*., 2018; Kudaykulov *et al*., 2019; Litvishko *et al*., 2020; Shen *et al*., 2019). To solve such problems, the authors propose a new numerical method for studying the thermomechanical state of a rod of the limited length from the heat-resistant alloy ANV-300, which allows one to take into account the dependence between the coefficient of thermal expansion and the field of temperature distribution, operating conditions, and fixing. Chemical composition in % for grade ANV-300: C (max 0.1), Si (max 0.5), Mn (max 0.5), Ni (64.2-70.1), S (max 0.01), P (max 0.015), Cr (14-17), W (7-10), Ti (1.4-2), Al (4.5-5.5), B (max 0.1), Ni – basis. It is used for the manufacture of ingots and cast rods intended for further remelting in the manufacture of shaped castings.

The determining fundamental relations of thermoelasticity of weakly compressible materials are considered in (Mikhlin, 1974; Lee *et al*., 2017; Pandiyan *et al*., 2019; Rabinskiy and Tushavina,

2019; Dmitriev *et al*., 2011; Kolokoltsev *et al*., 2020). Using a small parameter, an analytical solution to the problem of stretching a rod from a weakly compressible material under nonisothermal conditions is obtained. In (Nozdrev, 1967; Fedotov *et al*., 2018; Starovoitov *et al*., 2016; Qiu *et al*., 2017; Bartels, 2019; Krechetov *et al*., 2018; Civalek *et al*., 2020), the basic problems of thermodynamics and their application are described in sufficient detail. Zenkevich (1975) is devoted to the presentation of the finite element method, as one of the most effective methods for the numerical solution of engineering, physical and mathematical problems using computers. In (Timoshenko and Goodyear, 1975; Chen *et al*., 2017; Park *et al*., 2019; Hou and Gao, 2020; Santos *et al*., 2020), a systematic presentation of the theory of elasticity was given, starting with the derivation of the main relations and ending with some solutions obtained in recent years. The plane problem, the problem of torsion and stress concentration, some spatial problems, variational principles, and methods for solving problems are considered in detail.

Based on energy principles in combination with the use of a finite quadratic element with three nodes, a mathematical model, a computational algorithm, and a set of applied programs were developed in (Kudaykulov, 2009; Kudaykulov *et al*., 2009; Formalev *et al*., 2019; Formalev and Kolesnik, 2019; Myrzasheva and Shazhdekeyeva, 2015; Myrzasheva *et al*., 2016; Akhmetov and Kudaykulov, 2017; Myrzasheva *et al*., 2018; Deepa and Rajendran, 2018; Kuznetsova and Rabinskiy, 2019). With the help of these developments, the problems of determining the thermomechanical and thermo-stress-strain states of a rod of constant cross-section, depending on the presence of local thermal insulation, temperature, heat transfer, and their operating condition, are numerically solved. The mechanical properties of heat-resistant steels and alloys at room and high temperatures, the influence of alloying elements on the structure, and methods of thermal and hot processing of alloys are considered in (Himushin, 1969). Also considered are heat-resistant alloys on iron, nickel, cobalt bases, and several refractory metals and their alloys. The most important methods and techniques of computational mathematics are described in (Demidovich and Maron, 1960; Yano *et al*., 2018; Leon and Chen (Roger), 2019; Sun *et al*., 2020).

At present, in our republic and abroad, there are many scientific works devoted to the problem of determining the dependence of the thermally stressed-deformed state of bar elements of complex construction. Of these works, scientific studies by scientists of our country and neighboring countries can be noted: A.K. Kudaykulov (2009), B.B. Orazbaev (Orazbaev *et al*., 2017), M.M. Ermekov (2011), V.V. Afanasyeva (Afanasyeva and Lazerson, 1995), V.N. Bakulin (1985), I.A. Birger (1992), G.S. Pisarenko (Pisarenko *et al*., 1973), A.I. Oleinikov (Korobeinikov *et al*., 2008), Yu.A. Fedorov (2001), F.F. Himushin (1969) and others, as well as foreign scientists, like O. Zenkevich (1975), F. Krieth (1973), V.F. Nozdrev (1967), L. Segerlind (1979) and others.

2. MATERIALS AND METHODS

Consider a rod of limited length $L,(cm)$ made of the heat-resistant alloy ANV-300. Both ends of the shaft are rigidly pinched. The cross-sectional area of the rod is $F,(cm^2)$, which is constant over its entire length. The thermal expansion coefficient of the rod material $\alpha(T),\ (1/°K)$ depends on the field temperature distribution. The thermal conductivity coefficient of the rod material is $K_{xx},\left(\frac{watt}{cm\cdot °K}\right)$, the elastic modulus is $E,\left(\frac{kG}{cm^2}\right)$. The elastic modulus of the heat-resistant alloy ANV-300 is temperature independent. Through the cross-sectional areas of the two pinched ends of the rod, heat exchange occurs with their surroundings. For the left end of the rod $(x=0)$, the heat transfer coefficient is denoted by $h_0,\left(\frac{watt}{cm^2\cdot °K}\right)$, and the ambient temperature by $T_{amb\ 0},(°K)$. Similarly, for the right end $(x=L)$ – $h_L,\left(\frac{watt}{cm^2\cdot °K}\right)$ and $T_{amb\ L},(°K)$. Side surfaces, which are $\frac{1}{3}$ of the length of the rod, i.e., $(0\le x\le (L/3))$ and $((2L/3)\le x\le L)$ we consider the core to be thermally insulated. In the area of the rod $((L/3)\le x\le (2L/3))$, the local temperature is given. It can be constant, varying along the local length of the rod with linear and quadratic laws.

In the presence of heat sources due to thermal expansion and pinching, a stress-strain state appears in the inner sections of the rod. In this case, the components of the deformation and stress will be respectively, elastic $(\varepsilon_x,\ \sigma_x)$, temperature $(\varepsilon_T,\ \sigma_T)$ and thermoelastic $(\varepsilon,\ \sigma)$. If the field shows the temperature distribution and

thermal expansion coefficient along the length of the rod, then the expression of the function that characterizes the potential energy of elastic deformations of the considered rod has the following form (Equation 1), where V is the volume of the rod; Equation 2 is component of elastic deformation; Equation 3 is the field of elastic displacement along the length of the rod; Equation 4 is elastic component of stress; Equation 5 is the law distribution of the coefficient of thermal expansion along the length of the rod; E – module of elasticity of the core material; Equation 6 is law temperature distribution along the length of the rod.

To construct a mathematical model of the thermal stress state of a heat-resistant alloy rod pinched by two ends, we discretize it by quadratic elements with three nodes. Given that the process under consideration is a steady-state, within each discrete element, the field distribution of temperature, coefficient of thermal expansion and elastic displacement is approximated by a full second-order polynomial passing through three nodal points i, j and k (the length of the discrete element is λ, starting point *i*, mid-*j*, and finite-*k* and $x_i = 0$, Equations (7)-(8)). Within each discrete field element, the distribution of these functions is expressed by the following Equations (9)-(11) (Mikhlin, 1974; Nozdrev, 1967; Zenkevich, 1975). Where T_i, T_j, T_k are the values of $T(x)$ the nodal points *i, j, k*; u_i, u_j, u_k are the displacements of the sections along the coordinate, which are the coordinates of the nodes *i, j, k*, respectively; α_i, α_j, α_k are values of $\alpha(T(x))$ at these nodal points, respectively, in the interval $x \in (x_i \le x \le x_k)$; $\gamma_i(x), \gamma_j(x)$ and $\gamma_k(x)$ are the form functions for a quadratic element with three nodes, where (Equation 12).

The properties of these forms functions will ensure the continuity of the desired functions during the transition from one element to the next. For this case, the expression of the functional characterizing the potential energy of elastic deformation, in the presence of heat sources for one discrete element, has the following form (Equation 13). Where V_i is the volume of the discrete quadratic element under consideration with three nodes. Then the potential energy of elastic deformation of the entire rod in the presence of heat sources expressed as Equation 14. Where NDE is the number of discrete elements in the rod (Zenkevich, 1975; Timoshenko and Goodyear, 1975; Kudaykulov, 2009; Kudaykulov *et al*., 2009).

Considering each integral in expression (Equation 13) separately and from (Equation 12), finding the expression for partial derivatives $\frac{\partial \gamma_i}{\partial x}, \frac{\partial \gamma_j}{\partial x}$ u $\frac{\partial \gamma_j}{\partial x}$, and substituting them in Equation 13, we obtain an integrated expression of the function that characterizes the potential energy of elastic deformation of a discrete element in the presence of a temperature field (Equation 15). Further, minimizing the last functional concerning the nodal values of elastic displacement, we obtain a mathematical model of the thermally stressed state of a discrete element in the form of resolving systems of linear algebraic equations for the movement of element nodes (Equations 16-18).

These equations are obtained for nodes of one discrete element. Since we discretize the considered rod with a set of quadratic elements with three nodes, the expression for the functional of the potential energy of elastic deformation should be written for each element, taking into account the temperature field (Zenkevich, 1975; Myrzasheva and Shazhdekeyeva, 2015). Then, the general expression of potential energy for the considered rod as a whole has the form (Equation 14). The total number of nodes will be equal $2 \times nn + 1$. In the general case, the mathematical system of the thermally stressed state of the considered rod pinched by two ends is the following system of linear algebraic $2 \times nn + 1$ equation (19), where i is presented in the Equation 20. The displacement values of the two ends of the rod (due to rigid pinching) are equal to $u_1 = u_{2 \times nn + 1} = 0$.

Solving system (Equation 19), the nodal values of elastic displacements are determined. The values of the elastic component of the deformation in the first half of the element are determined as Equation 21. Similarly, for the second half of the element, we have (Equation 22). Accordingly, according to Hooke's law, the values of the elastic component of stress are determined as follows (Equation 23). The values of the temperature component of the deformation and stress are determined as follows (Equations 24-25). When ε_x^I; ε_x^{II}; ε_T^I; ε_T^{II}; σ_x^I; σ_x^{II}; σ_T^I; σ_T^{II} are known, values of thermoelastic strain and stress components are determined (Equations 26-27).

Based on the developed mathematical model, we will carry out a numerical simulation of the thermally stressed state of the considered rod in dependence $T_{amb\ 0}$, for fixed values of all other

parameters. The core works in the presence of heat transfer, thermal insulation, and temperature. The temperature varies along the local length of the rod by a linear law, i.e., (Equation 28) at $((L/3) \le x \le (2L/3))$, where (Equation 29). We coordinate the coordinate axis Ox from left to right (Figure 1). It is required to study the thermal stress state of a rod made of heat-resistant alloy ANV-300 clamped at both ends, depending on, for fixed values of all other parameters. Task. The values of the necessary parameters are as follows: $T_{amb\ 0} = T_{amb\ L} = 40\ (^\circ K)$. $a = 40$; $L = 30(cm)$; $T = 40x$; Equations (30)-(32) at $10 \le x \le 20(cm)$. We vary the value of the ambient temperature with the cross-sectional area of the left end $(x = 0)$ of the rod: $T_{amb\ 0} = 10\ (^\circ K);\ 20\ (^\circ K);\ 30\ (^\circ K);\ 40\ (^\circ K)$.

As mentioned above, in the presence of the given heat sources and partial thermal insulation, the rod tries to expand. However, due to the pinching of both ends, compressive forces R appear. In this regard, and due to the inhomogeneous temperature field, an inhomogeneous stress field arises in the inner sections of the rod. Components of the strain will be $\varepsilon_x, \varepsilon_T, \varepsilon$, and stresses $\sigma_x, \sigma_T, \sigma$. It is required to determine the displacement field (Equation 33), elastic deformations ε_x, temperature deformations ε_T, thermoelastic deformations ε, as well as elastic, temperature, and thermoelastic stresses σ_x, σ_T and σ.

To solve this problem, the considered rod is discretized $n = 150$ by quadratic elements with three nodes. Then the length of each element will be $\Delta\lambda = 0.2\,cm$. For each discrete element, an expression is written of the functional of the potential energy of elastic deformation, taking into account the presence of a temperature field. Next, summing them overall discrete elements, we find the expression of the corresponding functions for the considered rod as a whole. The total number of equations in the system will be $2n+1 = 301$. Since both ends of the rod are rigidly pinched, then $u_1 = u_{301} = 0$. In this regard, the number of equations in the system will be 299. By minimizing the potential energy of elastic deformation, taking into account the presence of a local field of temperature distribution and heat exchanges, we obtain (Equation 19), a system of resolving equations.

Moreover, if the number of discrete elements in the rod is n (where n is a positive integer), then the number of nodes in the rod will be $2n+1$. Nevertheless, since both ends of the rod are rigidly clamped, the movement of the extreme nodes will be zero, i.e. $u_1 = u_{2n+1} = 0$. Therefore, the minimization of the functional characterizing the potential energy of elastic deformations in the presence of a temperature field is minimized by nodal displacements (Equation 34). Solving the last system, we find the nodal values of displacement. Further, according to (Equations 21-27), the value of the components $\varepsilon_x, \varepsilon_T, \varepsilon$ $\sigma_x, \sigma_T, \sigma$ in the given sections of the rod are determined. The task (Equation 35) is accepted (Myrzasheva *et al*., 2016; Akhmetov and Kudaykulov, 2017).

3. RESULTS AND DISCUSSION:

To obtain the results of the problem, first it was considered the case when $T_{amb\ 0} = 10\ (^\circ K)$. In this case, the nodal values of the displacement are given in Table 1. The corresponding field distribution of displacement along the length of the considered rod is shown in Figure 2a). From this Table and the Figure, it can be seen that the sections of the rod that are on the site $0 < x < 24.85(cm)$ move against the direction of the axis Ox. Moreover, in this direction, the section with the coordinate $x = 13.2(cm)$ moves most. The value of the displacement of this section is $u_{132} = -0.03066239\ \ (cm)$. Cross-section of the rod, which are located on the site $24.85 < x < L = 30(cm)$, move in the direction of the axis Ox. In this case, a section whose coordinate is $x = 27.4(cm)$ moves more than other sections. The value of the displacement of this section is $u_{274} = 0.001973\ \ (cm)$. Comparing, we find that $|u_{132}| > |u_{274}|$.

The nodal values of the strain components of elastic ε_x, temperature ε_T and thermoelastic ε are respectively given in Tables 2 and 3. The field distribution of these strain components along the length of the considered rod is shown in Figure 3a). From these Tables and the Figure, it can be seen that the behavior of the elastic component of the deformation in the sections $0 < x \le 13.15(cm)$ and $27.35 \le x < L = 30(cm)$ of the rod will be compressive. However, in the area $13.15 < x < 27.35(cm)$ of the rod behaves tensile. The other two components of the deformation ε_T

and $\mathcal{E}$ along the entire length of the rod will have a compressive character. From Figure 3a), it is also seen that the field distribution of the components of elastic strains ε_x and thermoelastic strains $\mathcal{E}$ will be symmetric concerning a straight line whose equation is $\varepsilon = 0.0000033\ x - 0.0052$.

Nodal values of the component stresses of elastic σ_x, temperature σ_T , and thermoelastic σ are given in Tables 4 and 5. The corresponding field distribution of these component stresses is given in Figure 4a). From Tables 4 and 5, Figure 4a), it is seen that the behavior of the elastic component of the stress σ_x in the sections $0 < x \le 13.15(cm)$ and $27.35 \le x < L = 30(cm)$ of the rod will have a compressive character, and in the remaining sections of the rod σ_x behaves tensile. The remaining two components of stress σ_T, and σ along the entire length of the rod will have a compressive character. Also, it can be seen from Figure 4 that the distribution field σ_x and σ along the length of the considered rod will be symmetric for the straight line, the equation of which has the following form $\sigma = 9.304\,x - 10326.544$ (Himushin, 1969; Myrzasheva *et al*., 2018).

In the next step, increase the value $T_{amb\ 0}$, we accept $T_{amb\ 0} = 20\,(^\circ K)$. The corresponding displacement distribution field is shown in Figure 2b). From this graph, it can be seen that the cross-sections of the rod located on the coordinate plane section $0 < x \le 24.85(cm)$ move against the axis direction Ox . In this direction, the greatest displacement belongs to the coordinate section $x = 13.2(cm)$. The value is the displacement section of this section $u_{132} = -0.0305186\ \ (cm)$. The sections of the rod located on the site $24.85 < x < L = 30(cm)$ move in the direction of the axis Ox . In this case, the greatest displacement belongs to the point with the coordinate $x = 27.4(cm)$, and its largest value is $u_{274} = 0.001996\ \ (cm)$. This also shows that $|u_{132}| > |u_{274}|$.

The field distribution of the elastic ε_x, temperature ε_T and thermoelastic $\mathcal{E}$ deformation components along the length of the considered rod is shown in Figure 3b). From this figure, it is seen that the nature of the components of the deformation $\mathcal{E}_T$ and $\mathcal{E}$ along the entire length of the rod will be compressive. In contrast, their behavior of elastic deformations ε_x in the sections $0 < x \le 13.15(cm)$ and $27.35 \le x < L = 30(cm)$ the rod will be compressive, and in the remaining sections of the rod ε_x behaves in a tensile manner. It can also be seen from this figure that the field distribution of the strain components along the length of the considered rod will be symmetric to the straight line $\varepsilon = 0.0000033\ x - 0.0052$.

The field of distribution of elastic σ_x, temperature σ_T , and thermoelastic σ components of stress along the length of the considered rod is shown in Figure 4 b). In this case, the behavior of the components of the voltage σ_T and σ along the entire length of the rod will be compressive. In contrast, the nature of the behavior of the elastic component of the stress σ_x will be of a different kind. The elastic component of the stress σ_x is compressive in the sections of the rod $0 < x \le 13.15(cm)$ and $27.35 \le x < L = 30(cm)$, and in the remaining sections of the rod σ_x behaves in a tensile character. Figure 4b) also shows that this field, the distribution of the voltage components σ_x, and σ along the length of the considered rod will be symmetrical to the straight line, the equation of which has the following form $\sigma = 9.1128\,x - 10337.835$.

Now consider the case when $T_{amb\ 0} = 30\,(^\circ K)$. The corresponding displacement field along the length of the considered rod is given in Figure 2c). From this graph, the displacement field shows that the sections of the rod located on the coordinate plane plot $0 < x < 24.75\,(cm)$ move against the direction of the axis Ox , the largest displacement in this direction belongs to the point with the coordinate $x = 13.2(cm)$. The displacement value of this section is $u_{132} = -0.03037379\ \ (cm)$. The sections of the rod located on the site $24.75 < x < L = 30(cm)$ move in the direction of the axis Ox , the largest movement in this direction belongs to a point with a coordinate $x = 27.4(cm)$, whose value is $u_{274} = 0.0020191194\ \ (cm)$. It should also be noted that $|u_{132}| > |u_{274}|$.

The corresponding field distribution of the elastic ε_x, temperature $\mathcal{E}_T$, and thermoelastic $\mathcal{E}$ deformation components along the length of the

considered rod is shown in Figure 3 c). From these materials, it can be seen that the behavior of the elastic component of deformation ε_x in the sections $0 < x \le 13.15(cm)$ and $27.35 \le x < L = 30(cm)$ the rod will have a compressive character, and in the remaining sections of the rod ε_x behaves tensile. In contrast to elastic deformations ε_x, the behavior of the remaining components of the deformation ε_T and $\mathcal{E}$ along the entire length of the considered rod will have a compressive character. It can also be seen from this figure that the field distribution of the strain components along the length of the considered rod will be symmetric to the straight line $\varepsilon = 0.0000033\ x - 0.0052$.

The corresponding field of distribution of elastic, temperature σ_x, σ_T, and thermoelastic σ components of stresses is given in Figure 4c). From these results, it is clear that the behavior of the two-component stresses σ_T, and σ along the entire length of the rod will be compressive. In contrast, their elastic component of stress σ_x in the sections $0 < x \le 13.15(cm)$ and $27.35 \le x < L = 30(cm)$ the rod behaves compressive, and in the rest of it, it has a tensile character. From Figure 4c), it can also be observed that the field of distribution of the component voltages σ_x and σ are symmetric to a straight line, the equation of which has the following form $\sigma = 8.92x - 10349.218$. When the value $T_{amb0} = 40(°K)$ is varied, the corresponding field of the distribution of displacement, elastic, temperature, and thermoelastic components of the deformation $\varepsilon_x, \varepsilon_T$ and $\mathcal{E}$, σ_x, σ_T and σ stress along the length of the considered rod is given in Figures 2d), 3d), 4d) (Demidovich and Maron, 1960; Kudaykulov *et al.*, 2009).

By analyzing the studies of this problem by values $T_{amb\ 0} = 10\ (°K);\ 20\ (°K);\ 30\ (°K);\ 40\ (°K)$, we can construct the following comparative Table 6. These results show that in the case $T(x) = 40\ x$ at $(L/3) \le x \le (2L/3)$, the temperature changes with the surrounding cross-sectional area of the left end of the medium, i.e. T_{amb0}, minimal effect in comparison with h_0 the thermally stressed state of the investigated rod. Earlier, it was carried out a numerical study of the laws governing the influence of the heat transfer coefficient h_0 on the thermally stressed state of a rod at a temperature that varies linearly, taking into account $\alpha = \alpha(T(x))$. $\alpha = \alpha(T(x))$ – the law is the distribution of the coefficient of thermal expansion along the length of the rod, which expresses the full-scale dependence between the coefficient of thermal expansion and temperature. The rod is also made of heat-resistant alloy ANV-300 and pinched by two ends.

The laws of the fields of distribution of elastic displacements, component deformations, and stresses according to the values of the heat transfer coefficient $h_0 = 7.5;\ 10;\ 15;\ 30\ (watt/(cm^2 \cdot °K))$ are constructed. Based on the results of these studies, the following comparative table 7 is constructed.

4. CONCLUSIONS:

It was found that with increasing value h_0, the amplitude of displacements increases against the direction of the axis Ox, and the amplitude of displacements in the direction of the axis Ox decreases. With increasing value h_0, the maximum and average values of thermoelastic stress σ decreases.

Thus, it was established that only by changing the value h_0, (and not T_{amb0}), i.e., by changing the environmental properties of the surrounding cross-sectional area where heat transfer occurs, the thermally stressed state of the rod under investigation can be changed.

5. REFERENCES:

1. Afanasyeva, V.V., and Lazerson, A.G. (1995). Dynamic chaos in two-cavity klystron oscillators with delayed feedback. News of Universities. *Applied Nonlinear Dynamics*, *3*, 88-99.
2. Akhmetov, S., and Kudaykulov, A. (2017). On the method of construction of the dependence of the heat extension coefficient on the temperature in heat-resistant alloys. *International Journal of Engineering Research and Science (IJOER)*, *3*(8), 20-29.
3. Bakulin, V.N. (1985). *The finite element method for studying the stress-strain state of three-layer cylindrical shells*. Moscow, Russian Federation: TsSTI Information.
4. Bartels, S. (2019). Finite element simulation of nonlinear bending models for thin elastic rods and plates. Retrieved from https://arxiv.org/abs/1901.09835.
5. Birger, I.A. (1992). *Rods, plates, shells*.

Moscow, Russian Federation: Fizmatlit.

6. Chen, S.-K., Wan, C.-M., Liu, E.-H., Chu, S.-B., Liang, C.-Y., Yuan, L.-J. and Wan, C.-C. (2017). The microstructure of electrolytically deuterium-loaded palladium rods. Fusion Technology. *Fusion Technology*, *29*(2), 302-305.
7. Civalek, Ö., Uzun, B., Özgür Yaylı, M. and Akgöz, B. (2020). Size-dependent transverse and longitudinal vibrations of embedded carbon and silica carbide nanotubes by nonlocal finite element method. *The European Physical Journal Plus*, *135*, Article number 381.
8. Deepa, I.B., and Rajendran, V. (2018). Pure and Cu metal doped WO prepared via co-precipitation method and studies on their structural, morphological, electrochemical and optical properties. *Nano-Structures and Nano-Objects*, *16*, 185-192.
9. Demidovich, B.P., and Maron, I.A. (1960). *Fundamentals of computational mathematics*. Moscow, Russian Federation: Nauka.
10. Dmitriev, A.I., Skvortsov, A.A., Koplak, O.V., Morgunov, R.B., and Proskuryakov, I.I. (2011). Influence of the regime of plastic deformation on the magnetic properties of single-crystal silicon Cz-Si. *Physics of the Solid State*, *53*(8), 1547-1553.
11. Ermekov, M.M. (2011). *Collection and field preparation of oil and gas: textbook: for organizations of technical and vocational education*. Astana, Republic of Kazakhstan: Tome.
12. Fedorov, Yu.A. (2001). The choice of the design scheme of multilayer rods when calculating the temperature effect. In: B. Rymsza (Ed.), *10 rosyisko-polskie seminarium "Teoretyczne podstawy budownictwa" Moskwa-Iwanowo* (pp. 215-218). Warszawa, Poland: Oficyna Wydawnicza PW.
13. Fedotov, A.M., Murzakhmetov, A.N., and Dyusembaev, A.E. (2018). Expansion of ideas and processes in social and biological communities. *Eurasian Journal of Mathematical and Computer Applications, 6*(4), 17-28.
14. Formalev, V.F., and Kolesnik, S.A. (2019). Heat transfer in a half-space with transversal anisotropy under the action of a lumped heat source. *Journal of Engineering Physics and Thermophysics, 92*(1), 52-59.
15. Formalev, V.F., Kartashov, É.M., and Kolesnik, S.A. (2019). Simulation of nonequilibrium heat transfer in an anisotropic semispace under the action of a point heat source. *Journal of Engineering Physics and Thermophysics, 92*(6), 1537-1547.
16. Geng, J., Zhang, H., Mutuku, F., and Lee, N.-C. (2018). Novel solder alloy with wide service temperature capability for automotive applications. *International Symposium on Microelectronics*, *2018*(1), Article number 000075-000083.
17. Himushin, F.F. (1969). *Heat resistant steels and alloys* (2nd revised and enlarged edition). Moscow, Russian Federation: Metallurgy.
18. Hou, F., and Gao, Ch. (2020). Thermal effects analysis of end-pumped Er: YAG rod and slab by using finite element method. *International Conference on Optical Instruments and Technology: Advanced Laser Technology and Applications*, *11437*, Article number 1143709.
19. Kolokoltsev, V.M., Savinov, A.S., Andreev, S.M., and Angold, K.V. (2020). Calculation of a thermal stress state, when heating a steel cylindrical object. *Vestnik of Nosov Magnitogorsk State Technical University*, *18*(1), 37-45.
20. Korobeinikov, S.N., Oleinikov, A.I., Gorev, B.V., and Bormotin, K.S. (2008). Mathematical modeling of creep processes of metal products from materials having different tensile and compression properties. *Computational Methods and Programming: New Computational Technologies*, *9*(1), 346–365.
21. Krechetov, I.V., Skvortsov, A.A., Poselsky, I.A., Paltsev, S.A., Lavrikov, P.S., and Korotkovs, V. (2018). Implementation of automated lines for sorting and recycling household waste as an important goal of environmental protection. *Journal of Environmental Management and Tourism, 9*(8), 1805-1812.
22. Krieth, F. (1973). *Principles of heat transfer,* 3rd ed. New York City, New York: Futext Educational Publishers.
23. Kudaykulov, A., Arinov, E., Ispulov, N., Qadir, A., and Begaliyeva, K. (2019). *Numerical study of a thermally stressed state of a rod*. Retrieved from https://www.hindawi.com/journals/amp/2019/8986010/.
24. Kudaykulov, A.K. (2009). *Mathematical (finite*

element) modeling of applied problems of heat distribution in one-dimensional structural elements. Turkestan, Republic of Kazakhstan: Baiterek.

25. Kudaykulov, A.K., Myrzasheva, A.N., and Kenzhegulov, B.Z. (2009, June 30 – July 4) *Mathematical modeling of thermomechanical processes in pivotal element of the designs made from thermal stable infusible alloys*. Paper presented at the III Congress of the World Mathematical Society of Turkic-speaking Countries, Section No. 8, Mathematical Model, Almaty, Republic of Kazakhstan.
26. Kuznetsova, E.L., and Rabinskiy, L.N. (2019). Linearization of radiant heat fluxes in the mathematical modeling of growing bodies by the action of high temperatures in additive manufacturing. *Asia Life Sciences, 2*, 943-954.
27. Lee, T.-H., Ha, H.-Y., Jang, J.H., Kang, J.-Y., Moon, J.J., Park, Y., Lee, C.-H., and Park, S.-J. (2017). Self-twinning in solid-state decomposition. *Acta Materialia*, *123*, 197-205.
28. Leon, G., and Chen (Roger), H.-L. (2019). Direct determination of dynamic elastic modulus and poisson's ratio of Timoshenko rods. *Vibration*, *2*, 157-173.
29. Litvishko, V., Akhmetova, A., Kodasheva, G., Zhussupova, A., Malikova, R., and Kuralova, A. (2020). Formation of ecological education of the population. *E3S Web of Conferences, 159*, Article number 01009.
30. Mikhlin, S.G. (1974). *Variational-grid approximation*. Moscow Russian Federation: Nauka.
31. Myrzasheva, A.N., and Shazhdekeyeva, N. (2015). A numerical study of the dependence of the rod elongation on the ambient temperature, in the presence of a temperature that varies linearly. *Science and World. International Scientific Journal*, *1*(8(24)), 18-21.
32. Myrzasheva, A.N., Shambilova, G.K., and Shazhedekeeva, N.K. (2018). The temperature of the temperature of Bolshan Zhadayd rod termokerneulik kγyinің zhylu almasu coefficient keniinen tueldigin sandy қ zertteu ə zhene mathikalyқ modeldeu. *Bulletin of the Karaganda University, Mathematics Series, 1*(89), 84-89.
33. Myrzasheva, A.N., Shazhdekeyeva, N., and Tuleuova, R. (2016). Mathematical modeling of nonlinear thermomechanical processes in rods made of heat-resisting alloys. *International Journal of Pharmacy and Technology*, *8*(3), 17722-17732.
34. Nozdrev, V.F. (1967). *The course of thermodynamics*. Moscow, Russian Federation: Mir.
35. Orazbaev, B.B., Kenzhebaeva, T.S., Orazbaeva, K.N., Shzhedekeeva, N.K., and Myrzasheva, A.N. (2017). The study of sulfur processes at the Claus reactor and the development of models for assessing the quality of sulfur produced. *Vestnik of ENU*, *4*(119), 155-161.
36. Pandiyan, A., Arunkumar, G., and Premkumar, G. (2019). Design, analysis and topology optimization of a connecting rod for single cylinder 4–stroke petrol engine. *International Journal of Vehicle Structures and Systems*, *11*(4), 439-442.
37. Park, T.H., Woo, S.H., Lee, S.J., Sohn, D.M., Chung, C.K., Kim, Y.J., and Sohn, S. (2019). Cross-link is a risk factor for rod fracture at pedicle subtraction osteotomy site: A finite element study. *Journal of Clinical Neuroscience*, *66*, 246-250.
38. Pisarenko, G.S., Agaev, V.A. Kvitka, A.L., Popkov, V.G. and Umansky, E.S. (Eds.). (1973). *Resistance of materials*. Kiev, Ukraine: Publishing House "Higher School".
39. Qiu, Y., Young, M.L. and Nie, X. (2017). High strain rate compression of martensitic niti shape memory alloy at different temperatures. *Metallurgical and Materials Transactions A*, *48*, 601-608.
40. Rabinskiy, L.N., and Tushavina, O.V. (2019). Problems of land reclamation and heat protection of biological objects against contamination by the aviation and rocket launch site. *Journal of Environmental Management and Tourism, 10*(5), 967-973.
41. Santos, S.C., Rodrigues Jr., O., and Campos, L.L. (2020). Synthesis, processing and electron paramagnetic resonance response of YEuOmicro rods. *International Journal of Modern Physics: Conference Series*, *48*, Article number 1860112.
42. Segerlind, L. (1979). *Application of the finite element method*. Moscow, Russian Federation: Mir.
43. Shen, Z., Li, H., Liu, X., and Hu, G. (2019). Thermal-structural dynamic analysis of a satellite antenna with the cable-network and

hoop-truss supports. *Advances in Mathematical Physics*, *42*(11), 1339-1356.

44. Starovoitov, É.I., Leonenko, D.V., and Tarlakovskii, D.V. (2016). Thermal-force deformation of a physically nonlinear three-layer stepped rod. *Journal of Engineering Physics and Thermophysics*, *89*, 1582–1590.
45. Sun, G., Wu, M., Wu, J., and Chen, R. (2020). Experimental study on mechanical properties of 35CrMo-GLG650 steel rods at elevated temperatures. *Journal of Materials in Civil Engineering*, *32*(7), 239-247.
46. Timoshenko, S.P., and Goodyear, J. (1975). *Theory of elasticity*. Moscow, Russian Federation: Nauka.
47. Yano, T., Makoto, H., and Koichi, N. (2018). Effect of interfacial heat transfer on basic flow and instability in a high-Prandtl-number thermocapillary liquid bridge. *International Journal of Heat and Mass Transfer*, *125*, 1121-1130.
48. Zenkevich, O. (1975). *Method of finite elements in technology*. Moscow, Russian Federation: Mir.

$$\Pi = \int_V \frac{\sigma_x}{2} \varepsilon_x dV - \int_V \alpha\left(T(x)\right) \cdot E \cdot T(x) \cdot \varepsilon_x dV \quad \text{(Eq. 1)}$$

$$\varepsilon_x = \frac{\partial u}{\partial x} \quad \text{(Eq. 2)}$$

$$u = u(x) \quad \text{(Eq. 3)}$$

$$\sigma_x = E \cdot \varepsilon_x \quad \text{(Eq. 4)}$$

$$\alpha = \alpha\left(T(x)\right) \quad \text{(Eq. 5)}$$

$$T = T(x) \quad \text{(Eq. 6)}$$

$$x_j = \frac{\lambda}{2} \quad \text{(Eq. 7)}$$

$$x_k = \lambda \quad \text{(Eq. 8)}$$

$$T(x) = \gamma_i(x) \cdot T_i + \gamma_j(x) \cdot T_j + \gamma_k(x) \cdot T_k, \quad 0 \le x \le \lambda, \quad \text{(Eq. 9)}$$

$$\alpha(T(x)) = \gamma_i(x) \cdot \alpha_i + \gamma_j(x) \cdot \alpha_j + \gamma_k(x) \cdot \alpha_k, \; x \in (x_i \le x \le x_k) \quad \text{(Eq. 10)}$$

$$u(x) = \gamma_i(x) \cdot u_i + \gamma_j(x) \cdot u_j + \gamma_k(x) \cdot u_k \quad \text{(Eq. 11)}$$

$$\gamma_i(x) = \frac{\lambda^2 - 3\lambda x + 2x^2}{\lambda^2}; \; \gamma_j(x) = \frac{4(\lambda x - x^2)}{\lambda^2}; \; \gamma_k(x) = \frac{2x^2 - \lambda x}{\lambda^2}, \; 0 \le x \le \lambda \quad \text{(Eq. 12)}$$

$$\Pi_i = \int_{V_i} \frac{E}{2} \left(\frac{\partial u}{\partial x} \right)^2 dV - \int_{V_i} \alpha\left(T(x)\right) \cdot E \cdot T(x) \cdot \left(\frac{\partial u}{\partial x} \right) dV =$$

$$= \int_{V_i} \frac{E}{2} \left(\frac{\partial \gamma_i}{\partial x} u_i + \frac{\partial \gamma_j}{\partial x} u_j + \frac{\partial \gamma_k}{\partial x} u_k \right)^2 dV - \int_{V_i} E\left(\gamma_i \alpha_i + \gamma_j \alpha_j + \gamma_k \alpha_k\right)\left(\gamma_i T_i + \gamma_j T_j + \gamma_k T_k\right) \times$$

$$\times\left(\frac{\partial\gamma_i}{\partial x}u_i+\frac{\partial\gamma_j}{\partial x}u_j+\frac{\partial\gamma_k}{\partial x}u_k\right)dV \quad \text{(Eq. 13)}$$

$$\Pi=\sum_{i=1}^{NDE}\Pi_i \quad \text{(Eq. 14)}$$

$$\Pi_i=\frac{EF}{2}\left[\frac{7}{3\lambda}u_i^2-\frac{16}{3\lambda}u_iu_j+\frac{2}{3\lambda}u_iu_k+\frac{16}{3\lambda}u_j^2-\frac{16}{3\lambda}u_ju_k+\frac{7}{3\lambda}u_k^2\right]-$$
$$-EF\left\{\left[-\frac{1}{3}\alpha_iT_i-\frac{1}{5}\alpha_iT_j+\frac{1}{30}\alpha_iT_k-\frac{1}{5}\alpha_jT_i-\frac{8}{15}\alpha_jT_j+\frac{1}{15}\alpha_jT_k+\frac{1}{30}\alpha_kT_i+\right.\right.$$
$$\left.+\frac{1}{15}\alpha_kT_j+\frac{1}{15}\alpha_kT_k\right]u_i+\left[\frac{2}{5}\alpha_iT_i+\frac{4}{15}\alpha_iT_j+0+\frac{4}{15}\alpha_jT_i+0-\frac{4}{15}\alpha_jT_k+0-\right. \quad \text{(Eq. 15)}$$
$$\left.-\frac{4}{15}\alpha_kT_j-\frac{2}{15}\alpha_kT_k\right]u_j+\left[-\frac{1}{15}\alpha_iT_i-\frac{1}{15}\alpha_iT_j-\frac{1}{30}\alpha_iT_k-\frac{1}{15}\alpha_jT_i+\frac{8}{15}\alpha_jT_j+\right.$$
$$\left.\left.+\frac{1}{5}\alpha_jT_k-\frac{1}{30}\alpha_kT_i+\frac{1}{5}\alpha_kT_j+\frac{1}{3}\alpha_kT_k\right]u_k\right\}$$

$$\frac{\partial\Pi}{\partial u_i}=0;\Rightarrow\frac{EF}{2}\left[\frac{14}{3\lambda}u_i-\frac{16}{3\lambda}u_j+\frac{2}{3\lambda}u_k\right]-EF\left[-\frac{1}{3}\alpha_iT_i-\frac{1}{5}\alpha_iT_j+\frac{1}{30}\alpha_iT_k-\frac{1}{5}\alpha_jT_i-\right.$$
$$\left.-\frac{8}{15}\alpha_jT_j+\frac{1}{15}\alpha_jT_k+\frac{1}{30}\alpha_kT_i+\frac{1}{15}\alpha_kT_j+\frac{1}{15}\alpha_kT_k\right]=0 \quad \text{(Eq. 16)}$$

$$\frac{\partial\Pi}{\partial u_j}=0;\Rightarrow\frac{EF}{2}\left[-\frac{16}{3\lambda}u_i+\frac{32}{3\lambda}u_j-\frac{16}{3\lambda}u_k\right]-EF\left[\frac{2}{5}\alpha_iT_i+\frac{4}{15}\alpha_iT_j+\frac{4}{15}\alpha_jT_i-\frac{4}{15}\alpha_jT_k-\right.$$
$$\left.-\frac{4}{15}\alpha_kT_j-\frac{2}{5}\alpha_kT_k\right]=0 \quad \text{(Eq. 17)}$$

$$\frac{\partial\Pi}{\partial u_k}=0;\Rightarrow\frac{EF}{2}\left[\frac{2}{3\lambda}u_i-\frac{16}{3\lambda}u_j+\frac{14}{3\lambda}u_k\right]-EF\left[-\frac{1}{15}\alpha_iT_i-\frac{1}{15}\alpha_iT_j-\frac{1}{30}\alpha_iT_k-\frac{1}{15}\alpha_jT_i+\right.$$
$$\left.+\frac{8}{15}\alpha_jT_j+\frac{1}{5}\alpha_jT_k-\frac{1}{30}\alpha_kT_i+\frac{1}{5}\alpha_kT_j+\frac{1}{3}\alpha_kT_k\right]=0 \quad \text{(Eq. 18)}$$

$$\frac{\partial\Pi}{\partial u_i}=0 \quad \text{(Eq. 19)}$$

$$i=2\div(2\times nn-1). \quad \text{(Eq. 20)}$$

$$\varepsilon_x^I=\frac{\partial u}{\partial x}\left(x=\frac{x_j-x_i}{2}\right)=\frac{\partial u_i\left(x=\frac{x_j-x_i}{2}\right)}{\partial x}u_i+\frac{\partial u_j\left(x=\frac{x_j-x_i}{2}\right)}{\partial x}u_j+\frac{\partial u_k\left(x=\frac{x_j-x_i}{2}\right)}{\partial x}u_k. \quad \text{(Eq. 21)}$$

$$\varepsilon_x^{II} = \frac{\partial u}{\partial x}\left(x = \frac{x_k - x_j}{2} \right) = \frac{\partial u_i\left(x = \frac{x_k - x_j}{2} \right)}{\partial x} u_i + \frac{\partial u_j\left(x = \frac{x_k - x_j}{2} \right)}{\partial x} u_j + \frac{\partial u_k\left(x = \frac{x_k - x_j}{2} \right)}{\partial x} u_k \quad \text{(Eq. 22)}$$

$$\sigma_x^I = E \cdot \varepsilon_x^I ; \ \ \sigma_x^{II} = E \cdot \varepsilon_x^{II} \quad \text{(Eq. 23)}$$

$$\varepsilon_T^I = -\alpha\left(x = \frac{x_j - x_i}{2} \right) \cdot T\left(x = \frac{x_j - x_i}{2} \right) ; \ \varepsilon_T^{II} = -\alpha\left(x = \frac{x_k - x_j}{2} \right) \cdot T\left(x = \frac{x_k - x_j}{2} \right), \quad \text{(Eq. 24)}$$

$$\sigma_T^I = E \cdot \varepsilon_T^I ; \ \ \sigma_T^{II} = E \cdot \varepsilon_T^{II} . \quad \text{(Eq. 25)}$$

$$\varepsilon^I = \varepsilon_x^I + \varepsilon_T^I ; \ \varepsilon^{II} = \varepsilon_x^{II} + \varepsilon_T^{II} . \quad \text{(Eq. 26)}$$

$$\sigma^I = \sigma_x^I + \sigma_T^I ; \ \ \sigma^{II} = \sigma_x^{II} + \sigma_T^{II} \quad \text{(Eq. 27)}$$

$$T(x) = ax \quad \text{(Eq. 28)}$$

$$a = const > 0 \quad \text{(Eq. 29)}$$

$$K_{xx} = 100\left(\frac{watt}{cm \cdot °K} \right) \quad \text{(Eq. 30)}$$

$$h_L = 10\left(\frac{watt}{cm^2 \cdot °K} \right) \quad \text{(Eq. 31)}$$

$$E = 2 \cdot 10^6 \left(\frac{kG}{cm^2} \right) \quad \text{(Eq. 32)}$$

$$u = u(x) \quad \text{(Eq. 33)}$$

$$\frac{\partial \Pi}{\partial u_i} = 0, \ i = 2 \div 2n \quad \text{(Eq. 34)}$$

$$h_0 = h_L, \left(\frac{watt}{cm^2 \cdot °K} \right) \quad \text{(Eq. 35)}$$

Table 1. *Nodal values of displacement at* $T = 40x$; $T_{amb\ 0} = 10\ (^{\circ}K)$

Nodal point	$u\ [cm]$	Nodal point	$u\ [cm]$	Nodal point	$u\ [cm]$	Nodal point	$u\ [cm]$	Nodal point	$u\ [cm]$
1.	0.0000000000	…	…	…	…	…	…	…	…
2.	-0.0003794378	131.	-0.0306567073	247.	-0.0002250534	273.	0.0019694815	299.	0.0002668764
3.	-0.0007556759	132.	-0.0306623933	248.	-0.0000589692	274.	0.0019730125	300.	0.0001377738
…	…	133.	-0.0306563753	249.	0.0000952486	275.	0.0019654461	301	0.0000000000
		…	…	…	…	…	…		

Table 2. *Nodal values of* ε_x *at* $T = 40x$; $T_{amb\ 0} = 10\ (^{\circ}K)$

Nodal point	ε_x	Nodal point	ε_x	Nodal point	ε_x	Nodal point	ε_x	Nodal point	ε_x
1.	-0.0037943776	…	…	…	…	…	…	…	….
2.	-0.0037623810	130.	-0.0000646200	200.	0.0046474371	273.	0.0000353106	298.	-0.0012852206
3.	-0.0037602403	131.	-0.0000568600	201.	0.0046476582	274.	-0.0000756646	299.	-0.0012910264
…	…	132.	0.0000601800	202	0.0045233648	275.	-0.0000830244	300.	-0.0013777378
		…	…	…	….	…	…		

Table 3. *Nodal values of* ε_{II} *at* $T = 40x$; $T_{amb\ 0} = 10\ (^{\circ}K)$

Nodal points	ε	Nodal points	ε	Nodal points	ε
1.	-0.0065317029	…	…	…	…
2.	-0.0065317133	200.	-0.0138470109	298.	-0.0087514338
3.	-0.0065616728	201.	-0.0138500651	299.	-0.0086701528
…	…	202.	-0.0138500651	300.	-0.0086701528
		…	…		

Table 4. *Nodal values of* σ_x *at* $T = 40x$; $T_{amb\ 0} = 10\ (^\circ K)$

Nodal point	$\sigma_x\,[kG/cm^2]$	Nodal point	$\sigma_x\,[kG/cm^2]$	Nodal point	$\sigma_x\,[kG/cm^2]$	Nodal point	$\sigma_x\,[kG/cm^2]$	Nodal point	$\sigma_x\,[kG/cm^2]$
1.	-7588.7551487	…	…	…	…	…	…	…	…
2.	-7524.7620767	130.	-129.2400053	200.	9294.8741280	273.	70.6212747	298.	-2570.441200
3.	-7520.4806567	131.	-113.7200053	201.	9295.3164533	274.	-151.3291253	299.	-2582.052784
…	…	132.	120.3599947	202	9046.7295733	275.	-166.0488053	300.	-2755.475664
		…	…	…	…	…	…		

Table 5. *Nodal values of* σ_{II} *at* $T = 40x$; $T_{amb\ 0} = 10\ (^\circ K)$

Nodal points	$\sigma\,[kG/cm^2]$	Nodal points	$\sigma\,[kG/cm^2]$	Nodal points	$\sigma\,[kG/cm^2]$
1.	-13063.4058686485	…	…	…	…
2.	-13063.4266416485	200.	-27694.0218719856	298.	-17502.8676999818
3.	-13123.3456316485	201.	-27700.1301866520	299.	-17340.3055239819
…	…	202.	-27700.1301866521	300.	-17340.3055239819
		…	…		

Table 6. *Influence of ambient temperature on the stress-strain state of the test rod at different values* T_{amb0}

No.	$T_{amb\ 0}\,(^\circ K)$	$u_{\min}(cm)$	Coord.of the corres section (cm)	$u_{\max}(cm)$	Coord.of the corres section (cm)	$\sigma_{\max}\left(\frac{kG}{cm^2}\right)$	$\sigma_{midd}\left(\frac{kG}{cm^2}\right)$	Coord.of the corres section, where $u=0$ (cm)
1	10	-0.03066	$x=13.2$	0.001973	$x=27.4$	-27700.1	-19675.5	$x=24.85$
2	20	-0.03051	$x=13.2$	0.001996	$x=27.4$	-27717.1	-19707.4	$x=24.85$
3	30	-0.03037	$x=13.2$	0.002019	$x=27.4$	-27502.9	-19739.5	$x=24.75$
4	40	-0.03023	$x=13.2$	0.002042	$x=27.4$	-27751.5	-19771.9	$x=24.75$

Table 7. *The effect of the heat transfer coefficient on the stress-strain state of the investigated rod*

No.	$h_0\left(\frac{watt}{cm^2\cdot{}^\circ K}\right)$	$u_{\min}\,(cm)$	**Coord.of the corres section** (cm)	$u_{\max}\,(cm)$	**Coord.of the corres section** (cm)	$\sigma_{\max}\left(\frac{kG}{cm^2}\right)$	$\sigma_{midd}\left(\frac{kG}{cm^2}\right)$	**Coord.of the corres section, where** $u=0$ (cm)
1	7.5	-0.02946	$x=13.3$	0.00217	$x=27.1$	-27842.5	-19942.6	$x=24.65$
2	10	-0.03023	$x=13.2$	0.00204	$x=27.4$	-27751.5	-19771.9	$x=24.75$
3	15	-0.03125	$x=13.2$	0.001878	$x=27.4$	-27630.1	-19544.1	$x=24.95$
4	30	-0.0327	$x=12.9$	0.001656	$x=27.6$	-27459.6	-19224.6	$x=25.25$

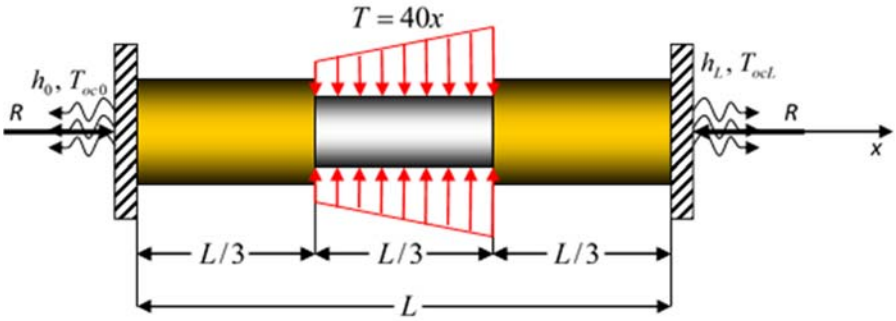

Figure 1. *The calculation scheme of the problem*

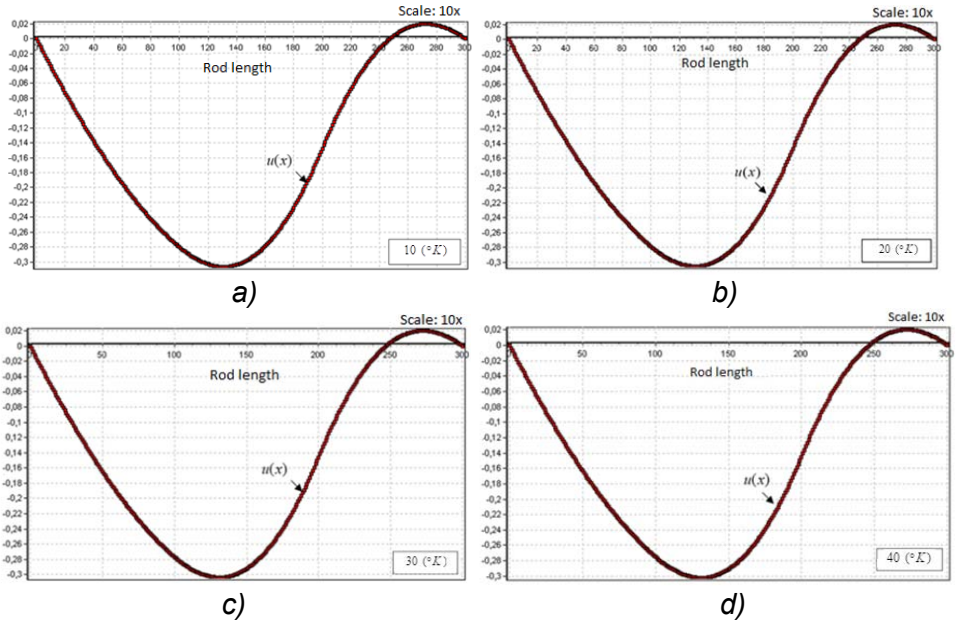

Figure 2. *Field distribution of elastic displacements along the length of the rod at* $T_{amb\ 0} = 10\,(^\circ K);\ 20\,(^\circ K);\ 30\,(^\circ K);\ 40\,(^\circ K)$

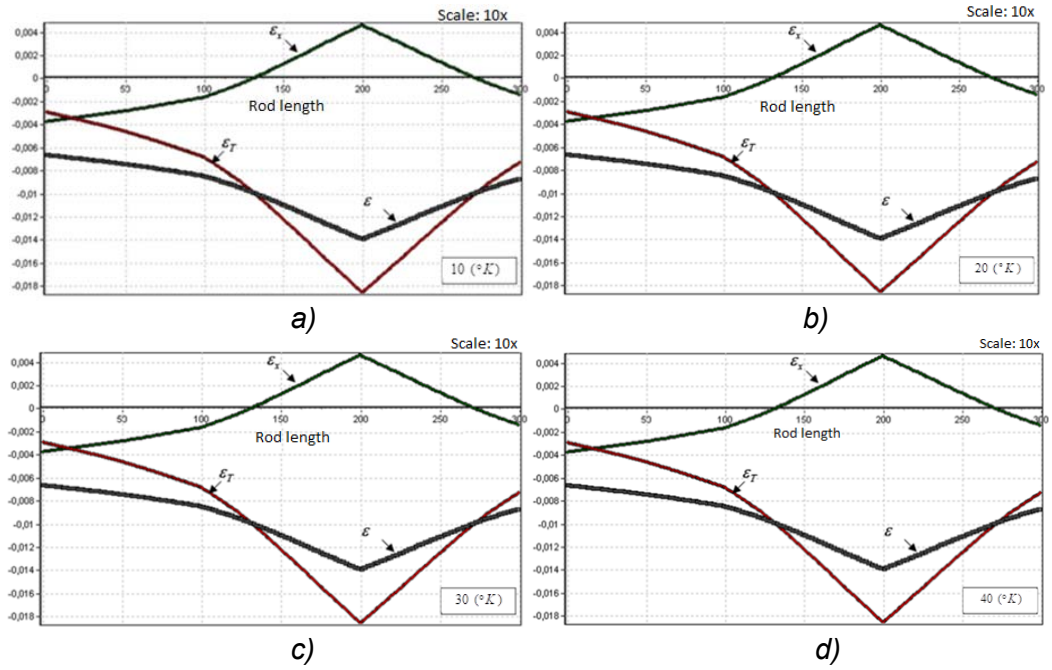

Figure 3. *Field distribution of deformations along the length of the rod at* $T_{amb\ 0} = 10\ (°K);\ 20\ (°K);\ 30\ (°K);\ 40\ (°K)$

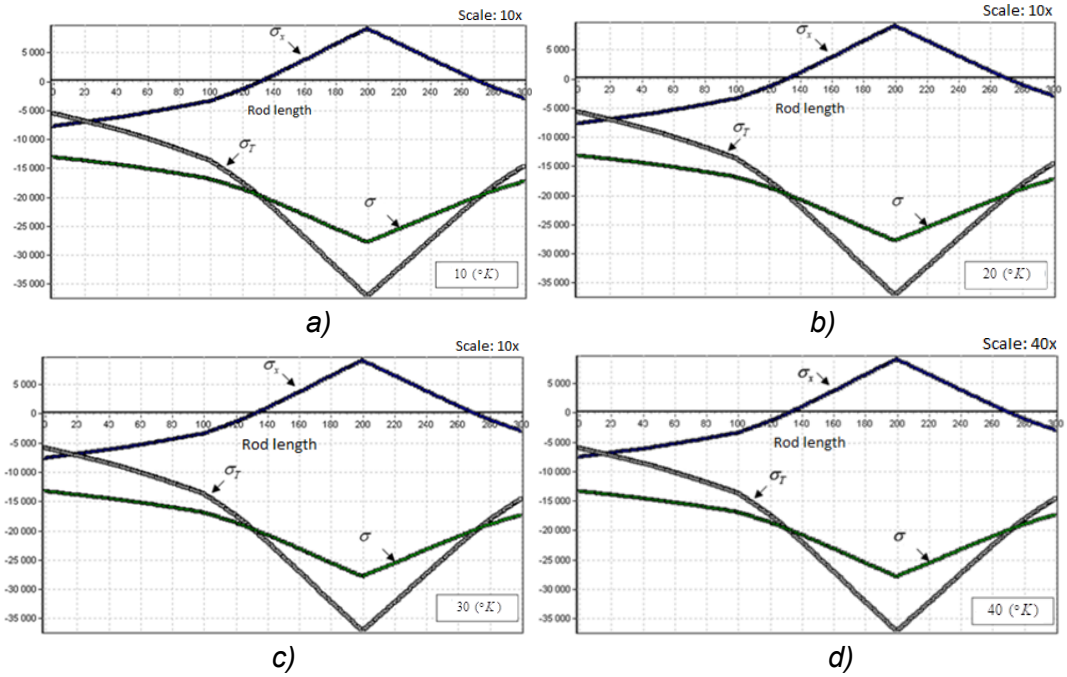

Figure 4. *Field stress distribution along the length of the rod at* $T_{amb\ 0} = 10\ (°K);\ 20\ (°K);\ 30\ (°K);\ 40\ (°K)$